Bull. Chem. Soc. Ethiop. **2025**, 39(7), 1301-1316.
DOI: https://dx.doi.org/10.4314/bcse.v39i7.6

ISSN 1011-3924
Printed in Ethiopia
Online ISSN 1726-801X

# COPPER(I) AND ZINC(II) COMPLEXES CONTAINING 4-METHOXYBENZ-ALDEHYDE THIOSEMICARBAZONE AND TRIPHENYLPHOSPHINE LIGANDS, SYNTHESIS, CHARACTERIZATION, AND THEORETICAL STUDIES

Karwan Omer Ali[1,2*], Nabil Adil Fakhre[1,3] and Salim Najm Aldain Saber[1]

[1]Department of Chemistry, College of Education, Salahaddin University-Erbil, Erbil 44001, Iraq
[2]Department of General Science, College of Basic Education, University of Halabja, Halabja 46018, Iraq
[3]Tishk International University, Erbil 44001, Iraq

(Received January 14, 2025; Revised March 16, 2025; Accepted March 18, 2025)

**ABSTRACT**. A new thioamide ligand, 4-methoxybenzaldehyde thiosemicarbazone (L), containing sulfur, nitrogen, and oxygen atoms, was synthesized via condensation of 4-methoxybenzaldehyde with thiosemicarbazide. New tetrahedral copper(I) and zinc(II) complexes of the prepared ligand and triphenylphosphine ($Ph_3P$) as a co-ligand have been synthesized. The ligand and its complexes were characterized by magnetic susceptibility, elemental analysis, molar conductivity, FT-IR, UV-Vis, and $^{1}H$, $^{13}C$, $^{31}P$-NMR techniques. The FT-IR spectra indicated that the (L) ligand coordinates with the metal ions through sulfur and nitrogen atoms, forming a five-membered chelate ring. Elemental analysis and $^{1}H$-NMR spectroscopy confirmed the mononuclear structure of complexes **2**, **3**, and **4**, while complex **1** exhibited a dinuclear configuration. DFT calculations indicated that the synthesized complexes are less thermodynamically stable than the free ligands, with ΔE values of 2.6776 eV, 2.9699 eV, 2.8912 eV, and 0.4996 eV for complexes **1**, **2**, **3**, and **4**, respectively. Among the complexes, complex **4** (S = 4.0032 eV) exhibited the highest softness, and all complexes were found to be softer compared to the free ligand. In this study, the results suggest that electron transitions in complexes are easier than in free ligands, which suggest their potential use in photocell technologies in the future.

**KEY WORDS**: Thioamide, Cu(I) complexes, Zn(II) complexes, NBO analysis, DFT calculations

## INTRODUCTION

In recent years, transition metal complexes ligated with thioamides have attracted considerable attention due to their pharmacological activities [1, 2]. Thioamide derivatives exhibit various biological behaviors, including antitumor, antifungal, antibacterial, antiviral, and anticarcinogenic activities [3]. Especially when derivatives of aromatic aldehyde are combined with thiosemicarbazide, novel thioamides are often synthesized with better pharmacological activities. [4]. The thioamide ligands contain multiple donor atoms, so they can form complexes with metal ions through either N or S atoms [5]. In general, they behave as chelating ligands for transition metal ions, ligated via sulfur (=S) and azomethine (=N-) groups; but, in certain cases, they are monodentate ligands, binding entirely through sulfur (=S) [6, 7]. X-ray crystallography indicated that the thiosemicarbazone ligands bind via the nitrogen and sulfur atoms, resulting in metal complexes with five-membered chelated rings [8]. In this work, Cu(I) and Zn(II) are selected as metal centers. Zinc is a vital trace mineral essential to numerous biological functions, and copper complexes have numerous pharmaceutical applications [9, 10]. The addition of triphenylphosphine, an organophosphorus substance, as a co-ligand also plays a critical role in coordination chemistry [11]. Because it has strong sigma-donor and pi-acceptor abilities, it can form stable complexes with a variety of metal ions [12]. There are a few papers describing metal complexes that combine both thioamide and triphenylphosphine ligands; however, researchers

*Corresponding authors. E-mail: karwan.ali@uoh.edu.iq

have thoroughly studied thioamide metal complexes separately [13]. An X-ray structure of a distorted tetrahedral copper(I) complex containing both 4-benzoylpyridinethiosemicarbazone and triphenylphosphine ligands has been reported [14]. Additionally, researchers synthesized and evaluated a distorted square planar copper complex containing salicylaldehyde thiosemicarbazone against colon (HCT-15) and pancreatic (PSN1) cancer cell lines using the MTT assay [15]. A study using X-ray crystallography showed that the $[Zn_2(L^{PhNO2})_2]$ complex (L = substituted nitrophenylbisthiosemicarbazone) has a distorted tetrahedral geometry [16].

The present study describes the synthesis, characterization, and geometrical structure of new Cu(I) and Zn(II) complexes containing 4-methylbenzaldehyde thiosemicarbazone ligand (L) and triphenylphosphine as co-ligands. These complexes were characterized by magnetic susceptibility, elemental analysis, molar conductivity, FT-IR, $^{31}P$, $^{1}H$, $^{13}C$-NMR, and UV-Vis techniques. In addition, theoretical studies, including FMO (Frontier Molecular Orbital), NBO (natural bond orbital), and MEP (molecular electrostatic potential), were conducted on the synthesized complexes.

## EXPERIMENTAL

### *Materials, general methods, and instrumentation*

Anhydrous $ZnCl_2$ and $CuCl_2.2H_2O$ were purchased from BDH, while triphenylphosphine was purchased from Carl Roth. Methanol (99%), dimethyl sulfoxide (99%), and dimethylformamide (99.5%) were supplied from Chem-Lab Company and used directly without further purification. FT-IR spectra were recorded using the Shimadzu FT-IR-Affinity-1 spectrophotometer within the range of 400–4000 $cm^{-1}$ using KBr discs. The far-infrared spectrum was obtained using a Shimadzu Affinity-ICE FTIR 800 $cm^{-1}$ spectrophotometer, operating in the 200-600 $cm^{-1}$ range utilizing CsI discs. UV-Vis spectra were measured utilizing a Jenway 7205 UV-Visible spectrophotometer with DMSO as the solvent. $^{1}H$, $^{13}C$, and $^{31}P$-NMR spectra were recorded on a Bruker 400 MHz Ultra-shield in DMSO-$d_6$ solvent at the University of Isfahan-Iran. In order to determine the carbon, hydrogen, nitrogen, and sulfur content of the synthesized ligand and its complexes, ECS 4010 at the University of Isfahan-Iran was utilized. The conductivity measurement was taken in a $10^{-3}$ M solution at 25 °C by using the Jenway 4200 conductivity/TDS meter. Magnetic susceptibility measurements were performed using the auto magnetic susceptibility Sherwood Scientific device. The melting point was measured using a melting device, model DMP-800, manufactured by A&E Lab UK CO., LTD.

### *Synthesis of 4-methoxybenzaldehyde thiosemicarbazone (L) ligand*

As shown in Scheme 1, the mixture of 4-methoxybenzaldehyde (0.680 g, 5.0 mmol) and thiosemicarbazide (0.456 g, 5.0 mmol) was refluxed in a mixture of distilled water (10 mL) and methanol (10 mL) as the solvent medium with the addition of (1-2 mL) glacial acetic acid. The reaction mixture was refluxed at 70 °C for 4 h. After that, the mixture was allowed to cool to room temperature, resulting in the appearance of a white precipitate. The precipitate was filtered, washed several times with cold ethanol, and recrystallized from absolute ethanol. White powder, Yield: 1.12 g (93.02 %), m.p. 173-174.5 °C. Anal. calc. for $C_9H_{11}N_3OS$ (M. wt. = 209.27 g/mol): C, 51.66; H, 5.3; N, 20.08; S, 15.32. Found: C, 51.88; H, 5.42; N, 20.23; S, 15.29 %. FT-IR (KBr, $cm^{-1}$) 3406, 3290 ($NH_2$), 3155 (NH), 3051 (C-H of aromatic ring), 2972, 2841 (C-H of $CH_3$), 1654 (C=N), 1606, 1448 (aromatic C=C), 1246 (C-O), 835 (C=S). $^{1}H$ NMR (400 MHz, DMSO-$d_6$) δ (ppm): 11.32 (s, 1H, NH), 7.99 (s. 1H, CH=N), 8.11, 7.91 (d, 2H, $NH_2$), 7.73 (d, 2H, $H_{2,6}$), 6.95 (d, 2H, $H_{3,5}$), 3.78 (s, 3H, O-$CH_3$). $^{13}C$-NMR (101 MHz, DMSO) (δ ppm): 177.61 (C=S), 160.71 (C-4), 142.29 (CH=N), 128.95 (C-2,6), 126.75 (C-1), 114.18 (C-3,5), 55.30 (O-$CH_3$). UV-Vis in DMSO [λ/nm, ($cm^{-1}$)]: 287 (34843), 357 (28011).

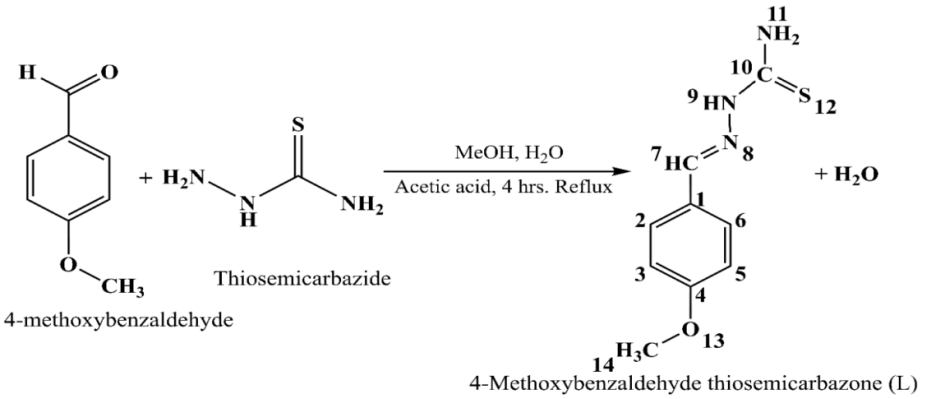


Scheme 1. Synthetic route of 4-methoxybenzaldehyde thiosemicarbazone (L) ligand.

*Synthesis of* $[Cu_2(\mu\text{-}Cl_2)(L)_2]$ ***1***. To a stirred solution of $CuCl_2.2H_2O$ (0.525 g, 3.08 mmol) in methanol (10 mL), a solution of (L) ligand (0.645 g, 3.08 mmol) in methanol (10 mL) was added dropwise. After that, the mixture was stirred for 1 h. at 50 °C, forming a green precipitate. The mixture was filtered off, and the precipitate was washed with methanol and dried in air. Yield: 0.957 g (81.79 %), m.p. 195-197 °C. Anal. calc. for $C_{18}H_{22}Cl_2Cu_2N_6O_2S_2$ (M. wt = 616.53 g/mol): C, 35.07; H, 3.60; N, 13.63; S, 10.40. Found: C, 35.64; H, 3.23; N, 13.91; S, 10.04 %. FT-IR (KBr, $cm^{-1}$) 3404, 3251 ($NH_2$), 3145 (NH), 3016 (C-H of aromatic ring), 2967, 2837 (C-H of $CH_3$), 1624 (C=N), 1604, 1423 (aromatic C=C), 1255 (C-O), 825 (C=S). $^1$H NMR (400 MHz, DMSO-$d_6$) δ (ppm): 11.80 (s, 1H, NH), 8.66, 8.56 (d, 2H, $NH_2$), 8.04 (s. 1H, CH=N), 7.82 (d, 2H, $H_{2,6}$), 7.76 (d, 2H, $H_{3,5}$), 3.75 (s, 3H, O-$CH_3$). UV-Vis in DMSO [λ/nm, ($cm^{-1}$)]: 288 (34722), 361 (27700), 415 (24096). Molar conductivity measurement: 8.3 $cm^2.ohm^{-1}.mol^{-1}$.

*Synthesis of* $[CuCl(L)(Ph_3P)]$ ***2***. A solution of (L) ligand (0.398 g, 1.90 mmol) in methanol (10 mL) was added dropwise to a stirring solution of $CuCl_2.2H_2O$ (0.324 g, 1.90 mmol) in methanol (10 mL). After 30 min of stirring, a green precipitate formed. Then, $Ph_3P$ (0.499 g, 1.90 mmol) in methanol (10 mL) was added, and the mixture was stirred for an additional 3 h, resulting in a yellow-green precipitate. The formed precipitate was filtered, washed with methanol, and dried in air. Yield: 1.06 g (86.60 %), m.p. 187-189.2 °C. Anal. calc. for $C_{27}H_{26}ClCuN_3OPS$ (M. wt = 570.55 g/mol): C, 56.84; H, 4.59; N, 7.36; S, 5.62. Found: C, 57.14; H, 4.13; N, 7.20; S, 5.13 %. FT-IR (KBr, $cm^{-1}$) 3410, 3280 ($NH_2$), 3149 (NH), 3072 (C-H of aromatic ring), 2983, 2837 (C-H of $CH_3$), 1624 (C=N), 1606, 1481 (aromatic C=C), 1435 (P-Ph), 1255 (C-O), 1095 (P-C), 827 (C=S). $^1$H NMR (400 MHz, DMSO-$d_6$) δ (ppm): 11.91 (s, 1H, NH), 8.80, 8.89 (d, 2H, $NH_2$), 8.07 (s. 1H, CH=N), 7.81 (d, 2H, $H_{2,6}$), 7.00 (d, 2H, $H_{3,5}$), 7.68-7.38 (m, 15H, $Ph_3P$), 3.80 (s, 3H, O-$CH_3$). $^{31}$P-NMR δ (ppm): δ = -3.93. UV-Vis in DMSO [λ/nm, ($cm^{-1}$)]: 288 (34722), 300 (33333), 364 (27472), 437 (22883). Molar conductivity measurement: 5.6 $cm^2.ohm^{-1}.mol^{-1}$.

*Synthesis of* $[Zn\ Cl_2(L)]$ ***3***. A solution of (L) ligand (0.662 g, 3.16 mmol) in methanol (10 mL) was added dropwise to a solution of $ZnCl_2$ (0.431 g, 3.16 mmol) in methanol (10 mL). Subsequently, the mixture was refluxed for 4 h, forming a clear solution. The clear solution was filtered and slowly evaporated at room temperature to yield a white precipitate. Yield: 0.987 g (90.30 %), m.p. 178-180 °C. Anal. calc. for $C_9H_{11}Cl_2N_3OSZn$ (M. wt = 345.55 g/mol): C, 31.28; H, 3.21; N, 12.16; S, 9.28. Found: C, 32.20; H, 2.96; N, 12.59; S, 8.83 %. FT-IR (KBr, $cm^{-1}$) 3433, 3284 ($NH_2$), 3180 (NH), 3078 (C-H of aromatic ring), 2980, 2837 (C-H of $CH_3$), 1633 (C=N), 1606, 1463 (aromatic C=C), 1247 (C-O), 829 (C=S). $^1$H NMR (400 MHz, DMSO-$d_6$) δ

(ppm): 11.40 (s, 1H, NH), 8.21, 7.85 (d, 2H, $NH_2$), 7.88 (s. 1H, CH=N), 7.74 (d, 2H, $H_{2,6}$), 6.96 (d, 2H, $H_{3,5}$), 3.81 (s, 3H, O-$CH_3$). UV-Vis in DMSO [λ/nm, ($cm^{-1}$)]: 295 (33898), 366 (27322). Molar conductivity measurement: 11.2 $cm^2.ohm^{-1}.mol^{-1}$.

*Synthesis of [ZnCl(L)($Ph_3P$)]Cl **4**.* To a solution of $ZnCl_2$ (0.260 g, 1.90 mmol) in methanol (10 mL), solid $Ph_3P$ (0.499 g, 1.90 mmol) was added. The mixture was then stirred at room temperature for 2 h. Following that, the (L) ligand (0.398 g, 1.9 mmol) was added, and the mixture was stirred for another 4 h, yielding a white precipitate. The formed precipitate was separated by filtration, washed with methanol, and dried in air. Yield: 1.06 g (91.61 %), m.p. 163.5-165.7 °C. Anal. calc. for $C_{27}H_{26}Cl_2N_3OPSZn$ (M. wt. = 607.84 g/mol): C, 53.35; H, 4.31; N, 6.91; S, 5.27. Found: C, 53.75; H, 3.95; N, 6.54; S, 5.03 %. FT-IR (KBr, $cm^{-1}$) 3433, 3286 ($NH_2$), 3178 (NH), 3057 (C-H of aromatic ring), 2980, 2837 (C-H of $CH_3$), 1635 (C=N), 1608, 1435 (aromatic C=C), 1435 (P-Ph), 1253 (C-O), 1103 (P-C), 828 (C=S). $^1$H NMR (400 MHz, DMSO-*d*6) δ (ppm): 11.38 (s, 1H, NH), 8.22, 7.84 (d, 2H, $NH_2$), 7.89 (s. 1H, CH=N), 7.74 (d, 2H, $H_{2,6}$), 6.96 (d, 2H, $H_{3,5}$), 7.68-721 (m, 15H, $Ph_3P$), 3.78 (s, 3H, O-$CH_3$). $^{31}$P-NMR δ (ppm): δ = -6.98. UV-Vis in DMSO [λ/nm, ($cm^{-1}$)]: 292 (34246), 312 (32051), 377 (26525). Molar conductivity measurement: 27.8 $cm^2.ohm^{-1}.mol^{-1}$.

*Computational details*

Density functional theory (DFT) calculations were performed with the Gaussian 09 software package to clarify the structure of the copper and zinc complexes. The Gauss View 6.0 software, with the B3LYP level of theory, was utilized to analyze the frontier molecular orbitals of the 4-Methoxybenzaldehyde thiosemicarbazone ligand and Cu(I) and Zn(II) complexes. The 6-311G basis set was employed for non-metal elements such as C, H, N O, S, P, and Cl, while the LANL2DZ basis set was utilized for the copper and zinc metal centres [17]. The molecular electrostatic potential (MEP) and natural bond orbital (NBO) calculations of the ligands and their complexes were carried out using the same Gaussian software [18].

## RESULTS AND DISCUSSION

Triphenylphosphine ($Ph_3P$) and 4-methoxybenzaldehyde thiosemicarbazone (L) were employed as ligands for the complexation of copper and zinc ions, as shown in Scheme 2. The reactions of equivalent amounts of $CuCl_2.2H_2O$ salt with 4-methoxybenzaldehyde thiosemicarbazone and $Ph_3P$ in methanol as solvent yielded complexes **1** and **2** as final products. In this reaction, the spontaneous reduction of Cu(II) to Cu(I) is caused by triphenylphosphine, which serves as a reducing agent. In addition, sterically demanding ligands containing sulfur also lead to the reduction process, which resulted in a colour change from blue to yellow-green. Nevertheless, in the reaction of anhydrous $ZnCl_2$ salt with 4-methoxybenzaldehyde thiosemicarbazone and $Ph_3P$ under specific experimental conditions, complexes **3** and **4** were synthesized as desired products. The structural composition of each complex was confirmed by elemental analysis, magnetic susceptibility, molar conductivity, UV-Vis, FT-IR, and $^1$H, $^{13}$C, $^{31}$P-NMR. The complexes dissolve in some organic solvents, such as dimethyl sulfoxide and dimethylformamide, at ambient temperature but not in ethanol, chloroform, acetone, diethyl ether, methanol, and water.

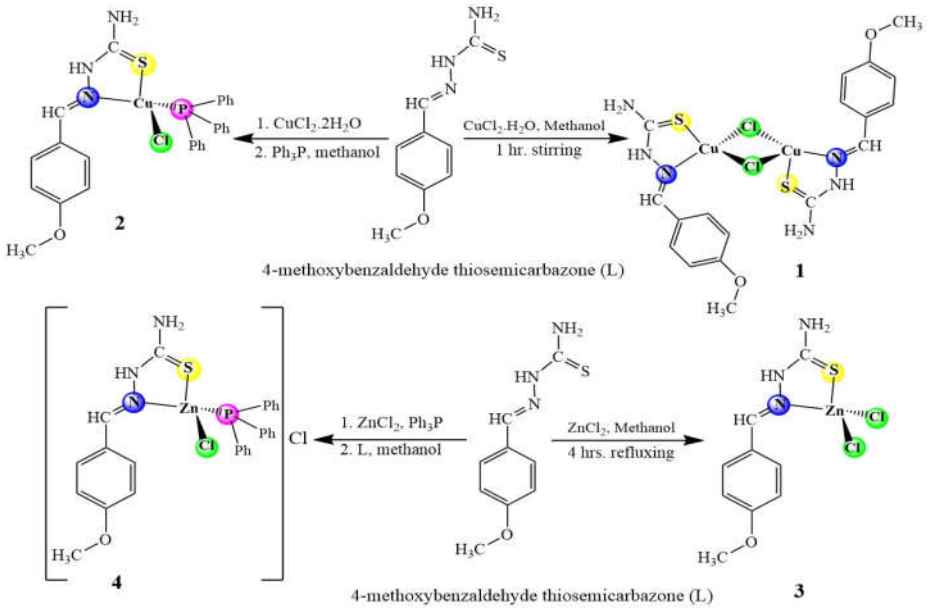


Scheme 2. Synthetic routes for complexes **1**, **2**, **3**, **1** and **4**.

*IR spectra*

The complexes were characterized by studying their infrared spectra and comparing them with the FT-IR spectra of the free ligands used in their synthesis. The IR spectrum of free ligand (L) exhibits medium bands of the -$NH_2$ group at 3406 and 3290 $cm^{-1}$, whereas the complex spectra of **1**, **2**, **3**, and **4** show medium bands of the -$NH_2$ group at (3404, 3251 $cm^{-1}$), (3410, 3280 $cm^{-1}$), (3433, 3284 $cm^{-1}$), and (3433, 3286 $cm^{-1}$), respectively [19]. The IR spectrum of the ligand shows the N-H band at 3155 $cm^{-1}$, and complexes have similar bands between 3145 and 3180 $cm^{-1}$, indicating the ligand remains as a thione tautomer in the solid state [20]. The free ligand has a characteristic $\nu$(C=N) band at 1654 $cm^{-1}$, but upon complexation, it was shifted to 1624, 1624, 1633, and 1635 $cm^{-1}$ in **1**, **2**, **3**, and **4**, respectively, indicating the participation of nitrogen in coordination with the corresponding metal ions. This is also supported by the appearance of new bands in the range of 638-646 $cm^{-1}$, which have been assigned to $\nu$(M-N) [21]. The band observed at 835 $cm^{-1}$ is related to $\nu$(C=S) in the IR spectrum of the ligand and is shifted towards a lower wave number in the IR spectra of the complexes. It suggests that thione sulfur is ligated to metal ions. Therefore, it can be concluded that the ligand acts as a bidentate chelating agent coordinated via azomethine nitrogen and thiolate sulfur [22]. The diagnostic of the $\nu$(P-Ph) band at 1435 $cm^{-1}$ supports the presence of coordinated triphenylphosphine. The new bands appearing in the range 304-340 $cm^{-1}$ are assigned to $\nu$(M-Cl) [23]. The assigned values of the significant IR spectral bands of the ligand and its metal complexes are collected in Table 1.

Table 1. The important IR frequencies ($cm^{-1}$) of $Ph_3P$, (L) ligands and complexes **1**, **2**, **3**, **4**.

| Assignments | **L** | **1** | **2** | **3** | **4** |
|---|---|---|---|---|---|
| *ν*(N-H$_2$) | 3406, 3290 | 3404, 3251 | 3410, 3280 | 3433 3284 | 3433, 3286 |
| *ν*(N-H) | 3155 | 3145 | 3149 | 3180 | 3178 |
| *ν*(C-H) aromatic | 3051 | 3016 | 3072 | 3078 | 3057 |
| *ν*(C-H) of CH$_3$ | 2972, 2841 | 2968, 2837 | 2983, 2837 | 2980, 2837 | 2980, 2837 |
| *ν*(C=N) | 1654 | 1624 | 1624 | 1633 | 1635 |
| *ν*(P-Ph) | - | - | 1435 | - | 1435 |
| *ν*(C-O) | 1246 | 1255 | 1255 | 1247 | 1253 |
| *ν*(C=S) | 835 | 825 | 827 | 829 | 828 |
| *ν*(M-N) | - | 640 | 646 | 642 | 638 |
| *ν*(M-S) | - | 526 | 526 | 466 | 470 |
| *ν*(M-Cl) | - | 340, 312 | 313 | 335, 310 | 304 |
| *ν*(M-P) | - | - | 371 | - | 362 |

*$^{13}C$, $^{1}H$, and $^{31}$P-NMR study*

The $^{13}$C NMR spectrum of the ligand (L) showed a peak at δ = 177.61 ppm attributed to the thione carbon (C=S), whereas the carbon (C-4) appeared at δ = 160.71 ppm. The imine carbon (C-7) appeared at δ = 142.29 ppm. The aromatic carbons (C-2,6), (C-1), and (C-3,5) showed signals at δ = 128.95, 126.75, and 114.18 ppm, respectively. The signal at δ = 55.3 (C-14) was assigned to the methyl group [24].

In the $^{1}$H-NMR spectrum of the free ligand (L), the (NH) proton appeared as a singlet signal at δ = 11.32 ppm. The protons of the ($NH_2$) group exhibited two distinct signals at δ = 8.11 and δ = 7.91 ppm, attributed to restricted rotation around the (C-$NH_2$) bond axis, resulting from delocalization of the lone pair of electrons on $NH_2$ nitrogen. The CH=N proton signal appears at δ = 7.99 ppm, and the methyl protons ($OCH_3$) at δ = 3.78 ppm. Aromatic protons exist as two doublets between 6.95 and 7.73 ppm [25]. A signal was detected between δ = 3.34-3.36 ppm, which is attributed to trace amounts of water in the DMSO solvent [26]. The spectra of complexes **1**, **2**, **3**, and **4** showed signals at δ 11.8, 11.91, 1140, and 11.38 ppm, respectively, corresponding to the N-H group, although this signal is slightly downfield shifted from that of the free ligand; the results are interpreted as evidence for (C=N) chelate formation (Figures S13-16). The (-CH=N-) protons are observed at δ 8.04, 8.07, 7.88, and 7.89 ppm for complexes **1**, **2**, **3**, and **4**, respectively [27]. The $^{1}$H-NMR spectral bands of the ligand and its metal complexes are collected in Table 2.

$^{31}$P-NMR spectra for complexes **2** and **4** exhibited a singlet signal at δP = -3.93 and -6.98 ppm, respectively, indicating the presence of a single isomer and showing the purity of the complexes [28].

Table 2. $^{1}$H-NMR data in (ppm) of (L) ligand and complexes **1**, **2**, **3**, **4**.

| Compounds | δ(N-H) | δ(N-H$_2$) | δ (HC=N) | δ(C-H) Aromatic | δ(C-H) $Ph_3P$ | δ($CH_3$) |
|---|---|---|---|---|---|---|
| **L** | 11.32 | 8.11, 7.91 | 7.99 | 7.746.95 | - | 3.78 |
| **1** | 11.80 | 8.66, 8.56 | 8.04 | 7.82-6.93 | - | 3.75 |
| **2** | 11.91 | 8.80, 8.59 | 8.07 | 7.81-6.98 | 7.68-7.38 | 3.80 |
| **3** | 11.4 | 8.21, 7.85 | 7.88 | 7.74-6.93 | - | 3.81 |
| **4** | 11.38 | 8.22, 7.84 | 7.89 | 7.74-6.94 | 7.68-7.21 | 3.80 |

*Electronic spectra, magnetic susceptibility and molar conductivity studies*

The UV-Visible spectra of triphenylphosphine ($Ph_3P$), 4-methoxybenzaldehyde thiosemicarbazone (L) ligands, and their corresponding complexes (**1**, **2**, **3,** and **4**) were recorded at room temperature in DMSO solution ($10^{-3}$ mol. $L^{-1}$), as shown in Figure 1. The $Ph_3P$ and thiosemicarbazone (L) ligands exhibited electronic absorption bands at 287 nm and 294 nm, attributed to $\pi \rightarrow \pi^*$ transitions, respectively. Also, the L ligand displayed an absorption band at 357 nm, which is associated with $n \rightarrow \pi^*$ transitions [29]. Complexes **1** and **2** exhibited absorption bands at 288 and 300 nm, as well as at 361 and 364 nm, attributed to intra-ligand transitions. The observed bathochromic shifts in these bands are due to the coordination of the ligands with the metal centers. Additionally, weak absorption bands were observed at 415 nm and 437 nm in compounds **1** and **2**, respectively, which are assigned to Metal-to-ligand charge transfer (MLCT) transitions [30]. The absorption spectra of Zn(II) complexes **3** and **4** displayed red-shifting of the ligand bands, indicating coordination of the ligands to the Zn(II) centers. These shifts are attributed to intraligand charge transfer transitions [31]. The Zn(II) metal complexes possess fully filled d orbitals, resulting in their diamagnetic character. The absence of d-d transitions, coupled with the presence of intraligand charge transfer, supports the proposed tetrahedral geometry for zinc complexes [32].

The complexes **1**, **2**, and **3** exhibited molar conductivity values in DMSO at 8.3, 5.6, and 11.2 $cm^2.ohm^{-1}.mol^{-1}$, respectively, indicating that they are non-ionic and have chlorine inside the coordination sphere [33]. In contrast, the complex **4** [Zn(L)($Ph_3P$)Cl]Cl showed a molar conductivity value of 27.8 $cm^2.ohm^{-1}.mol^{-1}$, suggesting the presence of only one chloride ion outside the coordination sphere, and the complex is ionic at a ratio equal to 1:1 [34].

All the complexes have ($\mu_{eff}$ < 1.0 B.M.) magnetic susceptibilities, which confirms that the complexes are tetrahedral and diamagnetic due to a filled $3d^{10}$ orbital of Zn(II) and Cu(I) metal ions [35, 36].

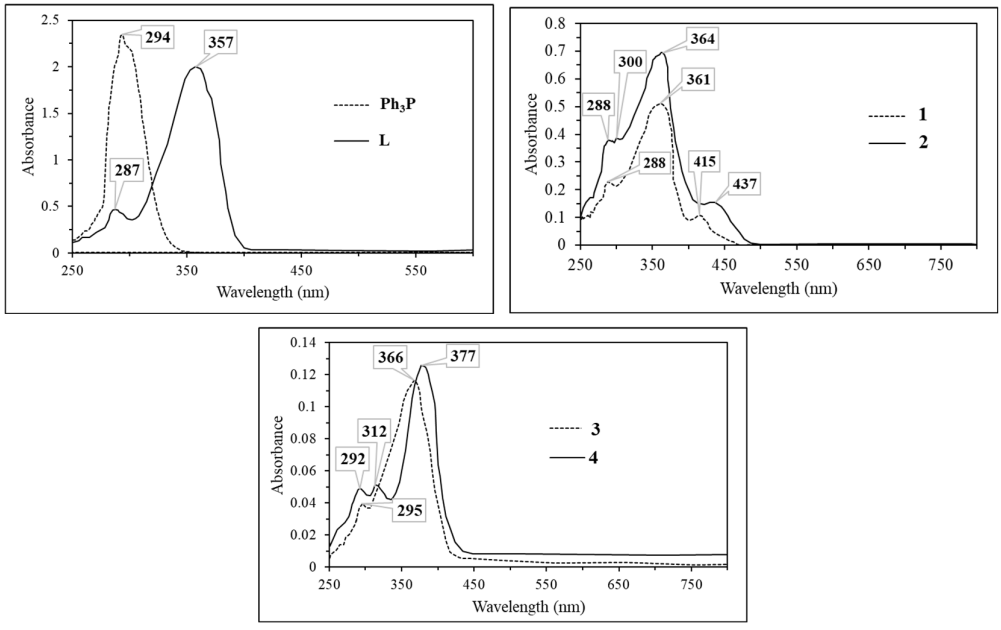


Figure 1. Electronic spectra of $Ph_3P$, (L) ligands and complexes **1**, **2**, **3**, and **4**.

*Theoretical studies*

Frontier molecular orbitals (FMOs) and their energy gaps are crucial parameters in quantum chemistry computations. Molecular reactivity and kinetic stability are demonstrated by FMO analysis. The chemical hardness of compounds can be used to determine their chemical stability. In general, molecules that are soft tend to be more polarizable since they require less energy to excite electrons from the HOMO to the LUMO. Hard molecules have a large energy gap, whereas soft molecules have a small energy gap [37]. In this study, we computed the electronic properties of the $Ph_3P$, 4-methoxybenzaldehyde thiosemicarbazone (L) ligands, and complexes **1**, **2**, **3**, and **4** using the B3LYP method and the 6-311G and LANL2DZ basis sets, respectively. The $Ph_3P$, L compounds, and complexes **1**, **2**, **3**, and **4** $E_{HOMO}$, $E_{LUMO}$, and ΔE energy gaps are presented in (Figures 2, 3). The quantum chemical parameters of the ligands and complexes are listed in Table 3. The free $Ph_3P$ and L ligands have an energy gap (ΔE) of 5.0121 and 3.3804 eV, while complexes **1**, **2**, **3**, and **4** have a ΔE of 2.6776, 2.9699, 2.8912, and 0.4996 eV, respectively. The results show that complex **4** is softer (S= 4.0032 eV) than the other complexes and ligands because it has the smallest energy gap (ΔE= 0.4996). Therefore, the synthesized Cu(I) complex **4** is more reactive and less stable than the other complexes. The chemical potential values for the synthesized complexes are negative, revealing that they are stable and do not decompose into their components. In addition, the electrophilicity index values for the complexes show that complex **4** is a stronger electrophile when compared with the other complexes [38].

Analysis of natural bond orbitals (NBOs) can be used to investigate intermolecular and intramolecular bonding, interactions between donors (ligands) and acceptors (metal centers), as well as charge transfer in molecular structures [39]. According to NBO analysis, the natural electron configuration (NEC) of Cu atoms in dinuclear complex **1** is $[Ar]4S^{0.33}\ 3d^{9.84}\ 4p^{0.16}\ 5p^{0.34}$ and $4S^{0.33}\ 3d^{9.83}\ 4p^{0.16}\ 5p^{0.35}$, containing 10.656 and 10.661 valence electrons and 0.00858 and 0.00872 Rydberg electrons. The natural charge of Cu atoms is +0.3377 and +0.3330e, supporting ligand-to-metal charge transfer. The occupancies of the Cu 3d orbitals are $d_{xy}^{1.9680}\ d_{xz}^{1.9689}\ d_{yz}^{1.9338}\ d_{X^2-Y^2}^{1.9782}\ d_{z^2}^{1.9868}$ and $d_{xy}^{1.9683}\ d_{xz}^{1.9712}\ d_{yz}^{1.9297}\ d_{X^2-Y^2}^{1.9770}\ d_{z^2}^{1.9871}$. The natural electron configuration (NEC) of the Cu atom in complex **2** is $[Ar]4S^{0.38}\ 3d^{9.81}\ 4p^{0.01}\ 5p^{0.82}$ containing 11.0034 valence electrons and 0.0152 Rydberg electrons. The Cu atom's natural charge is -0.0107e, which validates electron transfer to copper metal. The occupancy of the Cu 3d orbitals are $d_{xy}^{1.9339}\ d_{xz}^{1.9675}\ d_{yz}^{1.9842}\ d_{X^2-Y^2}^{1.9544}\ d_{z^2}^{1.9710}$. The NEC of the Zn atom in complex **3** is $[Ar]4S^{0.46}\ 3d^{9.98}\ 4p^{0.73}\ 5p^{0.01}$, containing 11.1677 valence electrons and 0.01630 Rydberg electrons [40]. The Zn atom's natural charge is +0.8159e, which validates electron transfer to zinc metal. The occupancy of the Cu 3d orbitals is $d_{xy}^{1.9954}\ d_{xz}^{1.9960}\ d_{yz}^{1.9964}\ d_{X^2-Y^2}^{1.9945}\ d_{z^2}^{1.9954}$. Also, the NEC of the Zn atom in complex **4** is $[Ar]4S^{0.43}\ 3d^{9.96}\ 4p^{0.01}\ 4d^{0.01}\ 5p^{0.29}$, containing 11.2216 valence electrons and 0.0159 Rydberg electrons. The natural charge of the zinc atom is +0.7623e, which indicates that electrons have been transferred to the zinc metal. The occupancy of the Cu 3d orbitals is $d_{xy}$ 1.9885 $d_{xz}$ 1.9913 $d_{yz}$ 1.9948 $d_{X^2-Y^2}^{1.9894}\ d_{z^2}^{1.9937}$. The NBO data indicates that the positive charge on the P (0.7610) atom in the free ligand decreases in complexes **2** and **4** due to the transfer of electron density from the filled metal's orbital to the empty orbital of the P atom (back bonding) [41].

The molecular electrostatic potential (MEP) surfaces for the ligands and their corresponding complexes were calculated and are shown in (Figure 4). In MEP surfaces, red regions indicate electrophilic reactivity, while blue regions represent nucleophilic reactivity [42]. The phosphorus atom in $Ph_3P$ and the sulfur atom in the (L) ligand, with their red regions, are identified as reactive sites for electrophilic attack due to the high electronegativity of these atoms. In all complexes, the chlorine atoms located at the negative electrostatic region represented by the red color are a good target for an electrophilic attack [43].

Table 3. Quantum chemical parameters (eV) and NBO Charges (e) of $Ph_3P$, (L) ligands and complexes **1**, **2**, **3**, and **4**.

| Parameter | **$Ph_3P$** | **L** | **1** | **2** | **3** | **4** |
|---|---|---|---|---|---|---|
| $E_{HOMO}$ | -5.7176 | -3.0082 | -4.4713 | -5.1859 | -6.3113 | -3.6267 |
| $E_{LUMO}$ | -0.7055 | 0.3722 | -1.7937 | -2.2160 | -3.4201 | -3.1271 |
| $\Delta E$ | 5.0121 | 3.3804 | 2.6776 | 2.9699 | 2.8912 | 0.4996 |
| I | 5.7176 | 3.0082 | 4.4713 | 5.1859 | 6.3113 | 3.6267 |
| A | 0.7055 | -0.3722 | 1.7937 | 2.2160 | 3.4201 | 3.1271 |
| η | 2.5061 | 1.6902 | 1.3388 | 1.4850 | 1.4456 | 0.2498 |
| S | 0.3990 | 0.5916 | 0.7469 | 0.6734 | 0.6918 | 4.0032 |
| χ | 3.2116 | 1.3180 | 3.1325 | 3.7010 | 4.8657 | 3.3769 |
| μ | -3.2116 | -1.3180 | -3.1325 | -3.7010 | -4.8657 | -3.3769 |
| ω | 2.0578 | 0.5139 | 3.6647 | 4.6120 | 8.1887 | 22.8252 |
| The NBO charge of $Ph_3P$, L ligands and their complexes | | | | | | |
| Atom | **$Ph_3P$** | **L** | **1** | **2** | **3** | **4** |
| Zn | - | - | - | - | 0.8159 | 0.7623 |
| Cu | - | - | 0.3377, 0.3330 | -0.0107 | - | - |
| Cl | - | - | -0.5200 | -0.4800 | -0.5736 | -0.4999 |
| Cl | - | - | -0.5140 | - | -0.6019 | - |
| N | - | -0.1095 | -0.3462, -0.3452 | -0.2991 | -0.3601 | -0.4035 |
| S | - | -0.1401 | 0.2440, 0.2400 | 0.25613 | 0.2388 | 0.2356 |
| P | 0.7610 | - | - | 0.5863 | - | 0.4290 |

Ionization potential ($I = -E_{HOMO}$); Electron affinity ($A = -E_{LUMO}$); Hardness ($\eta = (I - A)/2$); Softness ($S = 1/\eta$); Electronegativity ($\chi = (I + A)/2$); Chemical potential ($\mu = -(I + A)/2$); Electrophilicity ($\omega = \mu^2/2\eta$).

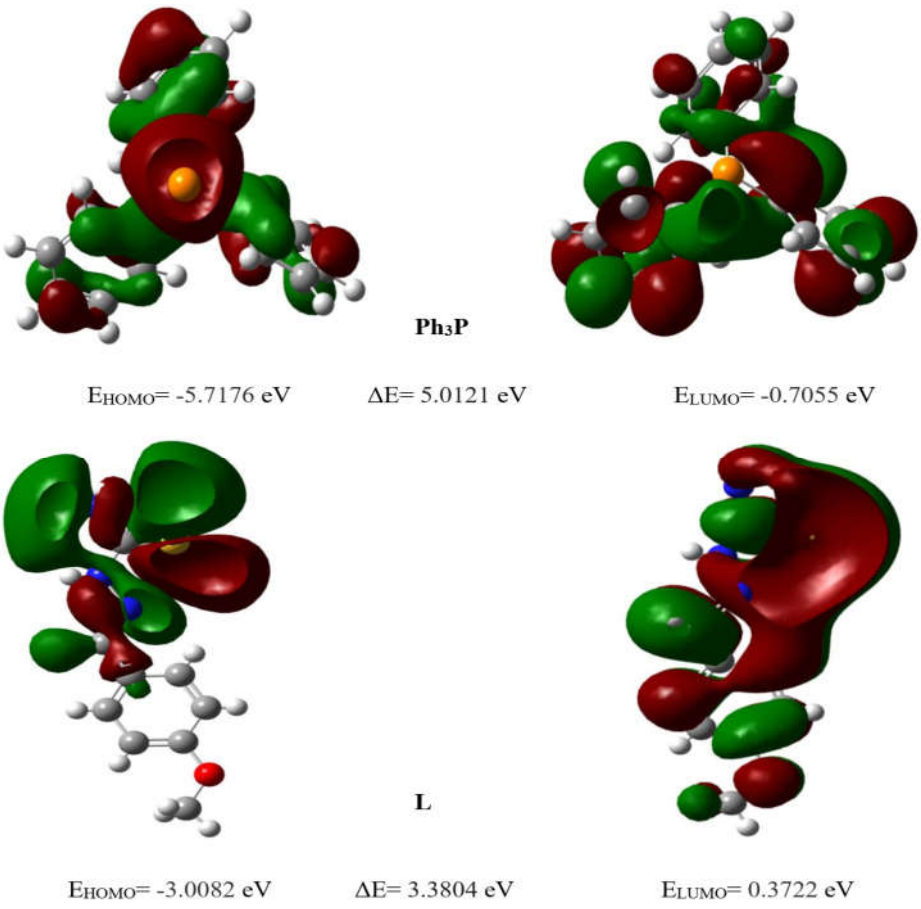


Figure 2. Surface plots of HOMO and LUMO orbitals of $Ph_3P$ and 4-methoxybenzaldehyde thiosemicarbazone (L) ligands.

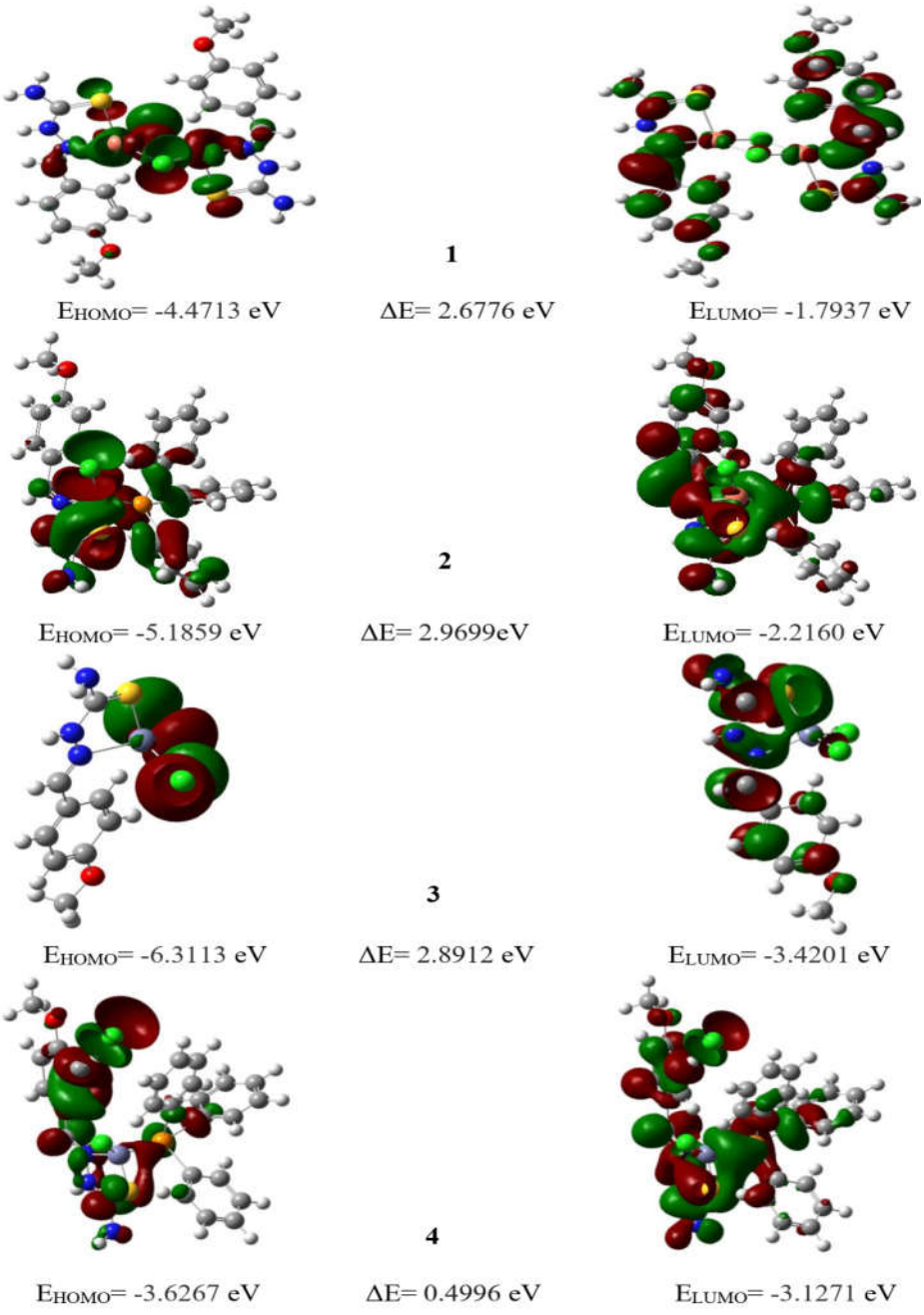


Figure 3. Surface plots of HOMO and LUMO orbitals of complexes **1**, **2**, **3**, and **4**.

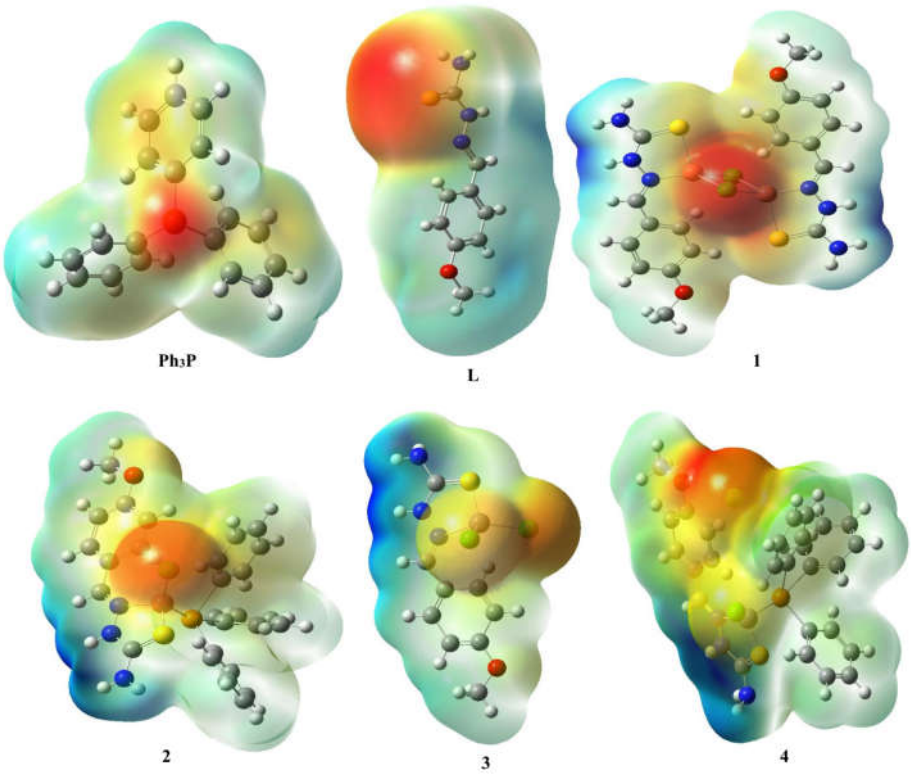


Figure 4. Molecular electrostatic potential (MEP) surfaces of $Ph_3P$, (L) ligands and complexes **1**, **2**, **3**, and **4**.

## CONCLUSION

This paper describes the synthesis and spectral characterization of $[Cu_2(\mu\text{-}Cl_2)(L)_2]$ **1**; $[CuCl(L)(Ph_3P)]$ **2**; $[ZnCl_2(L)]$ **3**; and $[ZnCl(L)(Ph_3P)]Cl$ **4** complexes containing thioamide and triphenylphosphine ligands. Spectroscopic studies demonstrate that the thioamide ligand (L) acts as a bidentate SN-donor. The data indicates that complexes **2**, **3**, and **4** are mononuclear, whereas complex **1** exhibits a dinuclear structure. The magnetic susceptibility measurements showed that the Cu(I) and Zn(II) complexes are diamagnetic due to a $d^{10}$ configuration. UV-Vis spectral analysis revealed metal-to-ligand charge transfer (MLCT) transitions at 415 and 437 nm in complexes **1** and **2**, respectively. Also, intraligand charge transfer transitions were observed at 366 and 377 nm in complexes **3** and **4**. The NBO analysis showed that the charge on the copper and zinc metals coordinated by the sulfur, nitrogen, and phosphorus atoms of the ligands (Cu = 0.3377 e **1**, Cu = -0.0107 e **2**, Zn = 0.8159 e **3**, and Zn = 0.7623 e **4**) is less than the formal charge of the $Cu^{+1}$ and $Zn^{+2}$ due to the transfer of electrons from the ligands to the metal centers.

## ACKNOWLEDGEMENT

The authors are grateful to the Chemistry Department of the College of Education at Salahaddin University for their assistance in the accomplishment of this study.

## REFERENCES

1. Kumar, R.R.; Ramesh, R.; Małecki, J.G. Versatile coordination ability of thioamide ligand in Ru(II) complexes: Synthesis, computational studies, in vitro anticancer activity and apoptosis induction. *New J. Chem.* **2017**, 41, 9130-9141.
2. Varna, D.; Geromichalou, E.; Hatzidimitriou, A.G.; Papi, R.; Psomas, G.; Dalezis, P.; Aslanidis, P.; Choli-Papadopoulou, T.; Trafalis, D.T.; Angaridis, P.A. Silver(I) complexes bearing heterocyclic thioamide ligands with $NH_2$ and $CF_3$ substituents: Effect of ligand group substitution on antibacterial and anticancer properties. *Dalton Trans.* **2022**, 51, 9412-9431.
3. Vekariya, M.K.; Patel, D.B.; Pandya, P.A.; Vekariya, R.H.; Shah, P.U.; Rajani, D.P.; Shah, N.K. Novel N-thioamide analogues of pyrazolylpyrimidine based piperazine: Design, synthesis, characterization, in-silico molecular docking study and biological evaluation. *J. Mol. Struct.* **2019**, 1175, 551-565.
4. Arshad, M.F.; Alam, A.; Alshammari, A.A.; Alhazza, M.B.; Alzimam, I.M.; Alam, M.A.; Mustafa, G.; Ansari, M.S.; Alotaibi, A.M.; Alotaibi, A.A.; Kumar, S. Thiazole: A versatile standalone moiety contributing to the development of various drugs and biologically active agents. *Mol.* **2022**, 27, 3994.
5. Lobana, T.S.; Sandhu, A.K.; Sultana, R.; Castineiras, A.; Butcher, R.J.; Jasinski, J.P. Coordination variability of $Cu^I$ in multidonor heterocyclic thioamides: Synthesis, crystal structures, luminescent properties and ESI-mass studies of complexes. *RSC Adv.* **2014**, 4, 30511-30522.
6. Aly, A.A.; Abdallah, E.M.; Ahmed, S.A.; Rabee, M.M; Bräse, S. Transition metal complexes of thiosemicarbazides, thiocarbohydrazides, and their corresponding carbazones with Cu(I), Cu(II), Co(II), Ni(II), Pd(II), and Ag(I)-A review. *Mol.* **2023**, 28, 1808-1847.
7. Abu-Dief, A.M.; Abdel-Rahman, L.H.; Shehata, M.R.; Abdel-Mawgoud; A.A.H. Novel azomethine Pd(II) and VO(II) based metallo-pharmaceuticals as anticancer, antimicrobial, and antioxidant agents: Design, structural inspection, DFT investigation, and DNA interaction. *J. Phys. Org. Chem.* **2019**, 32, e4009.
8. Mahmoudi, G.; Castiñeiras, A.; Garczarek, P.; Bauzá, A.; Rheingold, A.L.; Kinzhybalo, V.; Frontera, A. Synthesis, X-ray characterization, DFT calculations and Hirshfeld surface analysis of thiosemicarbazone complexes of $M^{n+}$ ions (n = 2, 3; M = Ni, Cd, Mn, Co and Cu). *Cryst. Eng. Comm*. **2016**, 18, 1009-1023.
9. Porchia, M.; Pellei, M.; Del Bello, F.; Santini, C. Zinc complexes with nitrogen donor ligands as anticancer agents. *Mol.* **2020**, 25, 5814-5855.
10. Hegde, P.L.; Bhat, S.S.; Revankar, V.K.; Shaikh, S.A.; Kumara, K.; Lokanath, N.K. Syntheses, structural characterization and evaluation of the anti-tubercular activity of copper(II) complexes containing 3-methoxysalicylaldehyde-4-methylthiosemicarbazone. *J. Mol. Struct*. **2022**, 1257, 132589.
11. Pann, J.; Roithmeyer, H.; Viertl, W.; Pehn, R.; Bendig, M.; Dutzler, J.; Kriesche, B.; Brüggeller, P. Phosphines in artificial photosynthesis: Considering different aspects such as chromophores, water reduction catalysts (WRCs), water oxidation catalysts (WOCs), and dyads. *Sustain. Energy Fuels* **2019**, 3, 2926-2953.
12. Brooner, R.E.; Brown, T.J; Widenhoefer, R.A. Synthesis and study of cationic, two-coordinate triphenylphosphine-gold-π complexes. *Chem. Eur. J.* **2013**, 19, 8276-8284.

13. Kumar, R.R.; Ramesh, R; Małecki, J.G. Ru(II) carbazole thiosemicarbazone complexes with four membered chelate ring: Synthesis, molecular structures and evaluation of biological activities. *J. Photoch. Photob. B: Biol.* **2016**, 165, 310-327.
14. Lobana, T.S.; Kaushal, M.; Bala, R.; Garcia-Santos, I.; Jasinski, J.P. Copper(I) derivatives of 4-benzoylpyridine thiosemicarbazone and 3-formylpyridine-N methylthiosemicarbazone with triphenylphosphine as a co-ligand. *J. Indian Chem. Soc.* **2022**, 99, 100298-100327.
15. Carcelli, M.; Tegoni, M.; Bartoli, J.; Marzano, C.; Pelosi, G.; Salvalaio, M.; Rogolino, D.; Gandin, V. In vitro and in vivo anticancer activity of tridentate thiosemicarbazone copper complexes: Unravelling an unexplored pharmacological target. *Eur. J. Med. Chem.* **2020**, 194, 112266-112315.
16. Fernández-Fariña, S.; Velo-Heleno, I.; Carballido, R.; Martínez-Calvo; M.; Barcia, R.; Palacios, Ò.; Capdevila, M.; González-Noya, A.M.; Pedrido, R. Exploring the biological properties of Zn(II) bisthiosemicarbazone helicates. *Int. J. Mol. Sci.* **2023**, 24, 2246-2262.
17. Orek, C.; Keser, S.; Kaygili, O.; Zuchowski, P.; Bulut, N. Structures and optical properties of zinc oxide nanoclusters: A combined experimental and theoretical approach. *J. Mol. Model.* **2023**, 29, 227.
18. Ali, K.O.; Mohamad, H.A.; Gerber, T.; Hosten, E. Zinc(II) complex containing oxazole ring: Synthesis, crystal structure, characterization, DFT calculations, and Hirshfeld surface analysis. *Acta Chim. Slov*. **2022**, 69, 7682-7690.
19. Alomar, K.; Khan, M.A.; Allain, M.; Bouet, G. Synthesis, crystal structure and characterization of 3-thiophene aldehyde thiosemicarbazone and its complexes with cobalt(II), nickel(II) and copper(II). *Polyhedron* **2009**, 28, 1273-1280.
20. Saleh, R.A.; Mahamad, H.A.; Al-Jibori, S.A. Pd(II) and Pt(II) mixed ligand complexes containing 2,5-dimercapto-1,3,4-thiadizole and 1,2-bis(diphenylphosphino)ethane ligands, synthesis, characterization, crystal structure, anticancer and computational studies. *Chem. Afr*. **2024**, 7, 1-13.
21. A Sadeek, S.; Mohamed, A.A.; Zordok, W.A.; Awad, H.M.; El-Hamid, A.; Mohamed, S. Spectroscopic characterization, thermogravimetric, DFT and biological studies of some transition metals complexes with mixed ligands of meloxicam and 1,10 phenanthroline. *Egypt. J. Chem.* **2021**, 64, 4197-4208.
22. Mohammed, M.M.; Hussein, M.B.; Sulfab, Y.; Adam, A.A.M. Synthesis, structural characterization and antimicrobial activity of new substituted oxazole thiosemicarbazone ligand and its Co(II) and Ni(II) complexes. *Sch. Int. J. Chem. Mater. Sci.* **2023**, 6, 75-84.
23. Mohamad, H.A.; Ali, K.O.; Gerber, T.A.; Hosten, E.C. Novel palladium(II) complex derived from mixed ligands of dithizone and triphenylphosphine synthesis, characterization, crystal structure, and DFT study. *Bull. Chem. Soc. Ethiop.* **2022**, 36, 617-626.
24. Al-Amiery, A.A.; Al-Azzawi, W.K.; Isahak, W.N.R.W. Isatin Schiff base is an effective corrosion inhibitor for mild steel in hydrochloric acid solution: Gravimetrical, electrochemical, and computational investigation. *Sci. Rep.* **2022**, 12, 17773-17791.
25. Ayoob, M.M.; Hawaiz, F.E.; Dege, N.; Kansız, S. Structural investigation and hirshfeld surface analysis of N-(3-chloro-4-methylphenyl)-2-(3-nitrobenzamido) benzamide. *J. Struct. Chem.* **2023**, 64, 1049-1058.
26. Ross, S.A.; Lowe, G. Downfield displacement of the NMR signal of water in deuterated dimethylsulfoxide by the addition of deuterated trifluoroacetic acid. *Tetrahedron Lett.* **2000**, 41, 3225-3227.
27. Chandra, S.; Bargujar, S.; Nirwal, R.; Yadav, N. Synthesis, spectral characterization and biological evaluation of copper(II) and nickel(II) complexes with thiosemicarbazones derived from a bidentate Schiff base. Spectrochim. *Acta A Mol. Biomol. Spectrosc*. **2013**, 106, 91-98.
28. Aziz, N.M.; Irzoqi, A.A. Synthesis, characterization, and biological evaluation of zinc(II) complexes with benzohydrazide derivative and phosphine ligands. *Bull. Chem. Soc. Ethiop.* **2025**, 39, 313-326.

29. Abd El-Hamid, S.M.; Sadeek, S.A.; Zordok, W.A.; El-Shwiniy, W.H. Synthesis, spectroscopic studies, DFT calculations, cytotoxicity and antimicrobial activity of some metal complexes with ofloxacin and 2, 2′-bipyridine. *J. Mol. Struct.* **2019**, 1176, 422-433.
30. Papazoglou, I.; Cox, P.J.; Papadopoulos, A.G.; Sigalas, M.P.; Aslanidis, P. Copper(I) complexes of 1,10-phenanthroline and heterocyclic thioamides: An experimental and theoretical (DFT) investigation of the photophysical characteristics. *Dalton Trans.* **2013**, 42, 2755-2764.
31. Chowdhury, T.; Bera, K.; Samanta, D.; Dolui, S.; Maity, S.; Maiti, N.C.; Ghosh, P.K.; Das, D. Unveiling the binding interaction of zinc(II) complexes of homologous Schiff-base ligands on the surface of BSA protein: A combined experimental and theoretical approach. *Appl. Organomet. Chem.* **2020**, 34, e5556.
32. Lakma, A.; Hossain, S.M.; van Leusen, J.; Kögerler, P.; Singh, A.K. Tetranuclear $Mn^{II}$, $Co^{II}$, $Cu^{II}$ and $Zn^{II}$ grid complexes of an unsymmetrical ditopic ligand: Synthesis, structure, redox and magnetic properties. *Dalton Trans.* **2019**, 48, 7766-7777.
33. Ghosh, K.; Kumar, P.; Mohan, V.; Singh, U.P. Self-activated DNA cleavage and nitric oxide reactivity studies on mononuclear copper complexes derived from tetradentate ligands. *Inorg. Chem. Commun.* **2012**, 15, 56-60.
34. Akouibaa, M.; Kadiri, M.; Driouch, M.; Tanji, K.; Ouarsal, R.; Rakib, S.; Sfaira, M.; Morley, N.; Lachkar, M.; El Bali, B.; Zarrouk, A. Synthesis, catalytic activity, magnetic study and anticorrosive activity of mild steel in HCl 1M medium of $(H_3dien)[Cu(NO_3)(C_2O_4)_2].2H_2O$. A redetermination at 100 K. *Mater. Chem. Phys*. **2023**, 307, 128130.
35. Singh, V.P.; Singh, P; Singh, A.K. Synthesis, structural and corrosion inhibition studies on cobalt(II), nickel(II), copper(II) and zinc(II) complexes with 2-acetylthiophene benzoylhydrazone. *Inorganica Chim. Acta* **2011**, 379, 56-63.
36. Abd El-Hamid, S.M.; Aziz, S.W.; Sadeek, S.A.; Sabry, M.A.; El-Gedamy, M.S. Synthesis, spectral analysis, XRD, molecular docking simulation of dithranol and glycine mixed ligand complexes and their potential role in suppressing breast cancer cells via down-regulating the expression of protein metalloproteinase-9. *Appl. Organomet. Chem*. **2024**, 38, p.e7650.
37. Sadeek, S.A.; Abd El-Hamid, S.M.; Mohamed, A.A.; Zordok, W.A.; El-Sayed, H.A. Spectroscopic characterization, thermogravimetry, density functional theory and biological studies of some mixed-ligand complexes of meloxicam and 2,2′-bipyridine with some transition metals. *Appl. Organomet. Chem*. **2019**, 33, p.e4889.
38. Li, Y.; Yang, Z.; Song, B.; Xia, H.; Wang, Z. Syntheses, crystal structures, and fluorescent studies of Cu(II) and Zn(II) complexes bearing 2-acetonaphthonebenzoylhydrazone ligand. *Inorg. Nano-Met. Chem.* **2017**, 47, 966-972.
39. Beheshti, A.; Bahrani-Pour, M.; Kolahi, M.; Shakerzadeh, E.; Motamedi, H.; Mayer, P. Synthesis, structural characterization, and density functional theory calculations of the two new Zn(II) complexes as antibacterial and anticancer agents with a neutral flexible tetradentate pyrazole-based ligand. *Appl. Organomet. Chem.* **2021**, 35, e6173.
40. Udaya Kumar, A.H.; Kumara, K.; Harohally, N.V.; Pampa, K.J.; Lokanath, N.K. Square planar trans-$N_2O_2$ Cu(II) complex: Synthesis, crystal structure, Hirshfeld surface, DFT, antimicrobial and docking studies. *ChemistrySelect* **2021**, 6, 6240-6255.
41. Saghatforoush, L.; Moeini, K.; Hosseini-Yazdi, S.A.; Mardani, Z.; Hajabbas-Farshchi, A.; Jameson, H.T.; Telfer, S.G.; Woollins, J.D. Theoretical and experimental investigation of anticancer activities of an acyclic and symmetrical compartmental Schiff base ligand and its Co(II), Cu(II) and Zn(II) complexes. *RSC adv.* **2018**, 8, 35625-35639.
42. Basak, T.; Bhattacharyya, A.; Das, M.; Harms, K.; Bauzá, A.; Frontera, A.; Chattopadhyay, S. Phosphatase mimicking activity of two zinc(II) Schiff base complexes with $Zn_2O_2$ cores: NBO analysis and MEP calculation to estimate non-covalent interactions. *ChemistrySelect* **2017**, 2, 6286-6295.

43. Abd El-Lateef, H.M.; Ali, A.M.; Khalaf, M.M.; Abdou, A. New Fe(III), Co(II), Ni(II), Cu(II), and Zn(II) mixed-ligand complexes: structural, DFT, biological, and molecular docking studies. *Bull. Chem. Soc. Ethiop*. **2024**, 38, 397-416.